Quasielastic neutrino scattering from oxygen and the atmospheric neutrino problem

J. Engel
Bartol Research Institute, University of Delaware, Newark, Delaware 19716

E. Kolbe and K. Langanke
W. K. Kellogg Radiation Laboratory, California Institute of Technology, Pasadena, California 91125

P. Vogel
Physics Department, California Institute of Technology, Pasadena, California 91125
(Received 23 April 1993)

We examine several phenomena beyond the scope of Fermi-gas models that affect the quasielastic scattering (from oxygen) of neutrinos in the 0.1–3.0 GeV range. These include Coulomb interactions of outgoing protons and leptons, a realistic finite-volume mean field, and the residual nucleon-nucleon interaction. None of these effects are accurately represented in the Monte Carlo simulations used to predict event rates due to μ and e neutrinos from cosmic-ray collisions in the atmosphere. We nevertheless conclude that the neglected physics cannot account for the anomalous μ-to-e ratio observed at Kamiokande and IMB, and is unlikely to change absolute event rates by more than 10–15 %. We briefly mention other phenomena, still to be investigated in detail, that may produce larger changes.

PACS number(s): 25.30.Pt, 13.15.Dk, 27.20.+n, 96.40.Tv

I. INTRODUCTION

For some years now, an apparent anomaly has existed in the numbers of μ- and e-type neutrinos reaching the Earth's surface after being produced in the atmosphere by cosmic rays [1, 2]. The observed ratio of muons to electrons created in water Čerenkov detectors is roughly 1:1, while simple facts about the decay of pions and kaons in the atmosphere lead one to expect a ratio much closer to 2:1. Although it is difficult to predict absolute fluxes for each kind of neutrino, errors tend to cancel in taking the ratio of the two. The roughly 2:1 expected ratio is robust, for example, against the $\approx 20\%$ uncertainties in our knowledge of cosmic-ray fluxes and cross sections. Furthermore, any errors in calculating lepton production in the detector are unlikely to appear in the ratio because a cut can be imposed on the momenta of the outgoing leptons. If momenta are restricted to values significantly above the mass of the muon, the cross sections for muon and electron production ought to be nearly identical.

The scattering of atmospheric neutrinos from oxygen is nonetheless worth investigating carefully. Even if details in the structure of ^{16}O do not affect the μ/e ratio, they may alter the total event rates considerably. A substantial change would have important consequences for the kinds of new physics that may be responsible for the anomaly. Monte Carlo simulations using the calculated fluxes of Refs. [3] and [4] imply that while roughly the correct number of e neutrinos are reaching the detector, far fewer μ neutrinos are arriving than expected. On the other hand, when the calculated fluxes of Ref. [5] are used the number of μ neutrinos appears to be correct, while too many electrons and positrons are produced. Attempts to resolve the problem [6–8] usually invoke the conversion of μ neutrinos into τ neutrinos on their way down from the top of the atmosphere. If the treatment of neutrino-oxygen scattering is not accurate, however, this explanation might not be viable. There may in fact be too many e neutrinos, as well as a shortage of μ neutrinos, no matter whose fluxes are correct; in that event μ-e oscillations (or some other new phenomenon such as proton decay [9]) will have to play a role. But theories incorporating these phenomena must then avoid existing constraints, e.g., from upward going muons [10] and solar neutrinos. In this paper, we attempt to shed some light on the situation through a careful examination of some aspects of the structure of ^{16}O that affect charge-exchange cross sections for GeV-range atmospheric neutrinos.

The experiments are able to identify outgoing particles by the nature of the Čerenkov rings they produce. By counting only "single-ring" events, experimenters can largely restrict the data to charged-current events in which electrons or muons are produced through quasielastic scattering (collisions that produce pions usually result in more than one ring). At both Kamiokande and IMB, variants of the relativistic Fermi-gas (RFG) model [11] are currently used to predict the scattering cross sections (see, e.g., Ref. [12]). It is not *a priori* obvious just how accurate the RFG model is in this context; it works well, for instance, in predicting electron-scattering cross sections at certain energies and angles [13], but fails to reproduce separated longitudinal and transverse responses [14–16]. A variety of effects [17] can modify the "free" RFG response (which usually mocks up binding effects through an average separation energy [11]), and

though they are not all completely understood, they need to be examined as thoroughly as possible in the context of neutrino scattering. Here we perform several calculations to test the role played by some of the physics not included in the Monte Carlo simulations of the detectors. Usually we will assume nonrelativistic nuclear kinematics, even though the incoming neutrinos can have energies up to a few GeV (we offer some justification for this below). To test the importance of each new effect, we therefore compare our results with those of the nonrelativistic Fermi-gas (NRFG) model. Fully relativistic nuclear models exist [18] and have been applied to quasielastic electron scattering [19,20], but are more complicated and less transparent than their nonrelativistic counterparts. Our implicit assumption is that relativistic treatments of new effects will result in corrections of the same order to the RFG model as do ours to the NRFG model.

The physics we assess includes the role played by bound states and resonances, the Coulomb interactions of the outgoing leptons and nucleons with the remaining A=15 nucleus, and the residual two-body interaction between nucleons in ^{16}O. The first two of these require a finite-volume model, which we develop in the next section. Interactions can be included in this model and (more schematically) in nuclear matter; we carry out both calculations in Sec. III. In Sec. IV we assess the cumulative effect of our results on atmospheric neutrino rates. Our conclusion is that while the new effects modify the rates to a degree and introduce some uncertainty, they do not dramatically alter the predictions of the RFG Monte Carlo simulations.

II. FERMI-GAS MODELS AND FINITE-VOLUME EFFECTS

The starting point for our investigation is the RFG model. Here, nucleons are Dirac spinors occupying plane wave states up to the nuclear Fermi momentum (for ^{16}O about 225 MeV/c), and carrying the same weak current as free nucleons. Nuclear binding is simulated by subtracting an average value $\overline{E}$ (about 27 MeV) from all occupied states; an energy transfer ω of at least $\overline{E}$ is required for any inelastic scattering. The RFG model was initially viewed as an unexpected success, in light of its simplicity, because it gave beautiful fits to early electron-scattering data [13]. As mentioned above, its shortcomings emerged only when transverse and longitudinal responses were measured separately [14–16]. The lack of total success in reproducing separated responses is significant in our context because the quasielastic neutrino response has a substantially larger transverse to longitudinal ratio than the (e,e') response at similar energies. The dominance of the transverse response is due largely to the axial-vector current, the "charge" component of which involves only the small components of the nucleon spinors.

We begin our quantitative study by citing Ref. [21], where the RFG model was studied and compared with other models for the scattering of neutrinos with energy below 300 MeV. One result of that work was a close agreement between total cross sections in the RFG and NRFG models, provided a semileptonic current-current interaction expanded to order $(q/M)^3$ was used in the latter. We have modified the treatment in Ref. [21] to include effects of order p/M in the current (these are quite small), and in addition have used completely nonrelativistic kinematics to facilitate later comparison with potential-model calculations. We find, as shown in Table I, that even at the energies important for atmospheric neutrino scattering the agreement between the RFG and NRFG models (with the same values for the Fermi momentum and average binding, and folded with the Kamioka neutrino flux [3]) remains reasonably good. That this is not preposterous can be seen from Fig. 1, where the distribution in energy transfer ω is displayed for representative values of the outgoing lepton momentum. Because of the steep drop with energy of the atmospheric neutrino spectrum [3] a substantial part of the scattering occurs at low enough ω so that a nonrelativistic treatment makes qualitative sense. As already noted, we will consequently examine other effects in the context of nonrelativistic models. We will continue, however, to use the usual relativistic dipole nucleon form factors with the standard cutoff values M_V = 0.84 GeV, M_A = 1.032 GeV, the usual CVC (conserved vector current) form of the weak magnetism term, and the Goldberger-Triemann relation for the induced pseudoscalar term. In addition we use the neutrino fluxes of Ref. [3] everywhere below, and as a measure of event rates for a given lepton momentum we employ and expression for the total "yield" given by

TABLE I. Ratios of the lepton yields calculated in the RFG and NRFG models, and the absolute $(\mu^- + \mu^+)$ and $(e^- + e^+)$ yields in units of 10^{-41} (s MeV)$^{-1}$ in the RFG model.

p (MeV/c)	μ^-	μ^+	e^-	e^+	$\mu^- + \mu^+$	$e^- + e^+$	Yield (μ)	Yield (e)
150	0.95	1.05	0.94	1.02	0.96	0.95	6.80	4.29
250	1.06	1.03	1.05	1.01	1.06	1.04	9.35	5.56
350	1.15	1.01	1.14	1.00	1.13	1.12	7.40	4.12
450	1.15	1.00	1.15	0.99	1.12	1.11	5.37	2.85
550	1.14	0.98	1.13	0.97	1.10	1.10	3.97	2.07
650	1.12	0.96	1.12	0.96	1.08	1.07	3.02	1.55
750	1.10	0.94	1.10	0.93	1.05	1.05	2.35	1.20
850	1.07	0.91	1.08	0.91	1.03	1.03	1.87	0.94
950	1.06	0.90	1.07	0.90	1.01	1.02	1.51	0.76

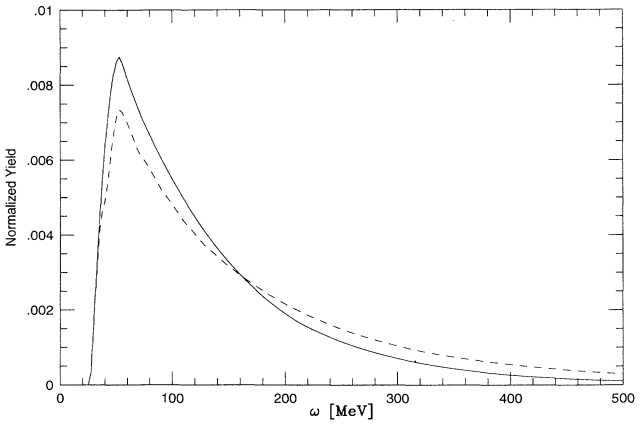

FIG. 1. Contribution in the RFG model of different energy transfers ω to the $\mu^- + \mu^+$ yield for muon momenta of 250 MeV/c (solid curve) and 550 MeV/c (dashed curve).

$$Y(p_{\rm lep}) = \int_{E_{\rm lep}}^{\infty} \frac{d\sigma(E_\nu)}{dp_{\rm lep}} f(E_\nu)\, dE_\nu \ , \tag{2.1}$$

where $E_{\rm lep} = E_\nu - \omega$ and $f(E_\nu)$ is the incoming neutrino (or antineutrino) flux.

The Fermi-gas model treats a nucleus such as ^{16}O as if it were nuclear matter with a slightly reduced density. Within such a context it is difficult to incorporate the physics of bound states, resonances, and Coulomb repulsion, which derive from the finite extent of the nucleus. The steep drop in the neutrino flux (reflected in Fig. 1) ought to enhance these features; to begin to understand their role we model ^{16}O as eight protons and eight neutrons occupying the lowest three levels of a standard Wood-Saxon potential

$$V(r) = -V_0 f(r) + V_{ls} \frac{1}{r} \frac{df}{dr} \boldsymbol{l} \cdot \boldsymbol{s} \ , \tag{2.2}$$

where

$$f(r) = \{1 + \exp[r - R]/a\}^{-1} \ , \tag{2.3}$$

and R, a are measures of the nuclear radius and diffuseness. The final states consist of both bound and continuum eigenstates of the same potential. Corrections to the weak current up to order $(q/M)^3$, p/M are included in the same way as in our version of the NRFG model. A similar picture of neutrino scattering was presented several years ago [22], but did not consider the effects of lepton mass, or use a current with corrections beyond $1/M$.

Unfortunately the finite-well model described above will not necessarily yield more accurate results than the Fermi-gas model. As is shown in Ref. [23], the average excitation energy at a given momentum transfer q in a local potential (which must also be spin independent—not the case here) must be the same as in the Fermi-gas model with *no* binding added. A shift can only arise from a nonlocal potential or a two-body interaction. This is not entirely surprising because a local energy-independent potential is not an accurate representation of the mean nuclear field. A better model is the optical potential, which is known to be energy dependent or, equivalently, nonlocal. To some extent the average binding energy inserted in the Fermi-gas model simulates the effects of two-body interactions or of a nonlocal mean field.

We nonetheless use the simple single-particle potential model outlined above as a starting point to which all kinds of additional physics can be added. To indicate the relation between this picture and the NRFG model, we show the ratio of yields in the two models in the first half of Table II. Our Wood-Saxon potential is specified by V_0=51 MeV, V_{ls}=32.8 MeV fm^2, R=1.27$A^{1/3}$, a=0.65 fm. As shown in Table II, for $p_{\rm lep} \leq 550$ MeV/c the potential model leads to slightly higher yields than the NRFG model. We attribute this to the Wood-Saxon single-particle bound states and resonances, the effects of which should be most pronounced at low lepton momentum.

TABLE II. The yield ratios of $\mu^- + \mu^+$ and $e^- + e^+$ between the one-body Wood-Saxon (WS) potential model and the NRFG model (columns 2 and 3) and, within the Wood-Saxon model, the ratio of yields with and without Coulomb interactions (columns 4 and 5).

p (MeV/c)	NRFG/WS		With/without Coulomb for protons in WS model	
	$\mu^- + \mu^+$	$e^- + e^+$	$\mu^- + \mu^+$	$e^- + e^+$
150	1.05	1.04	0.95	0.95
250	1.10	1.10	0.97	0.97
350	1.09	1.09	0.97	0.97
450	1.04	1.04	0.97	0.97
550	1.02	1.01	0.97	0.97
650	0.99	0.99	0.97	0.97
750	0.96	0.96	0.97	0.97
850	0.94	0.95	0.97	0.97
950	0.93	0.94	0.98	0.98

To incorporate the proton-nucleus Coulomb interaction, we alter the potential felt by outgoing protons by adding a repulsive interaction associated with a spherical volume of uniformly distributed charge. As pointed out in Ref. [24], the use of different interactions for initial and final states spoils vector-current conservation; the magnitude of the problem, however, is small. The second part of Table II shows the effect of Coulomb repulsion on the outgoing protons, which are produced only by incoming neutrinos (i.e., not by antineutrinos). In accord with intuition, the repulsive Coulomb interaction reduces their yield. When the contribution of neutrinos and antineutrinos are added, however, the magnitude of the reduction, shown in the table, is only about 3%.

Within the Wood-Saxon model we can also examine the Coulomb interaction of the outgoing charged lepton with the nucleus. It is tempting to treat the interaction as is commonly done for nuclear β decay, i.e., by multiplying the cross section by a Fermi function $F(Z,p)$:

$$F(Z,p) = \frac{|\psi_{\rm Coul}(r=R)|^2}{|\psi_{\rm plane\ wave}(r=R)|^2} \rightarrow \frac{\pm 2\pi Z\alpha}{1-\exp(\mp 2\pi Z\alpha)} , \tag{2.4}$$

where Z is the nuclear charge, α is the fine structure constant, R is the nuclear radius, and the limit is for ultrarelativistic electrons and muons ($p/E \rightarrow 1$). This procedure, however, is valid only for outgoing s-wave particles; it clearly cannot be applicable more generally since the ultrarelativistic limit is not unity, as it ought to be. In our case, because pR can be much greater than 1, we need a better procedure. Guided by distorted-wave analysis of quasielastic electron scattering [23], we replace the momentum of the charged outgoing lepton by an effective value

$$p_{\rm eff} = p\left(1+\frac{\langle V\rangle}{E}\right) , \quad \langle V\rangle = \pm\frac{4Z\alpha}{3R} , \tag{2.5}$$

when evaluating the nuclear matrix element. ($\langle V\rangle$ is the mean value of the Coulomb potential inside the nucleus.) The Coulomb correction treated in this way turns out to be very small, on the order of 1%.

III. RESIDUAL INTERACTION

So far the models we have considered do not explicitly incorporate residual two-body interactions between nucleons. The Fermi-gas models, with the extra 27 MeV binding, simulate their effects to some degree, but it is not obvious whether a more realistic treatment of the interactions will change event rates significantly. In this section, we examine this question first for illustration in the context of nuclear matter, that is, as explicit two-body corrections to the no-binding NRFG, and then more rigorously in the finite-volume model. In both instances we will use the one tried and (reasonably) true method for calculating continuum response: the random phase approximation (RPA).

In nuclear matter the calculation is straightforward [25]. The quasielastic response is related to the particle-hole "polarization" propagator in a medium, which can be approximately evaluated as a sum of ring diagrams. For the relevant part of the interaction, we use the standard $\pi+\rho+\delta$-function parametrization of the two-body particle-hole potential, i.e. (in momentum space),

$$V_{ph} = (f_0' + V_\pi + V_\rho)\,\tau_1\cdot\tau_2 , \tag{3.1}$$

$$V_\pi = J_\pi(\omega,q)\left[g_0' + \frac{q^2}{\omega^2-q^2-m_\pi^2}\right]\sigma_1\cdot\hat{\mathbf{q}}\sigma_2\cdot\hat{\mathbf{q}} ,$$

$$V_\rho = J_\pi(\omega,q)\left[g_0' + \frac{J_\rho(\omega,q)}{J_\pi(\omega,q)}\frac{q^2}{\omega^2-q^2-m_\rho^2}\right] \times(\sigma_1\times\hat{\mathbf{q}})\cdot(\sigma_2\times\hat{\mathbf{q}}) ,$$

where $f_0' = 0.6/m_\pi^2$, $g_0' = 0.7$, and

$$J_\pi = 4\pi\frac{f_{\pi NN}^2}{m_\pi^2}F_\pi^2(\omega,q) , \; J_\rho = 4\pi\frac{f_{\rho NN}^2}{m_\rho^2}F_\rho^2(\omega,q) . \tag{3.2}$$

The π and ρ coupling strengths $f_{\pi NN}$ and $f_{\rho NN}$, and the form factors F_π and F_ρ are defined in Ref. [26], which also contains many relevant references. The spin-singlet force is a pure (Landau-Migdal) contact force, while in the spin-triplet channel, the two terms correspond to π and ρ exchange supplemented by a phenomenological contact force (softened by pion form factor) to approximately account for short range correlations. Though we have used couplings that appear commonly in the literature, no consensus exists on the values these parameters take in a medium; a simultaneous reproduction of high-q electron-scattering and p-p data has so far proved elusive. We will therefore also consider as an alternative a pure density-dependent Landau-Migdal interaction commonly used to describe low-energy excitations in finite nuclei [27].

Figure 2 shows cross sections for production of elec-

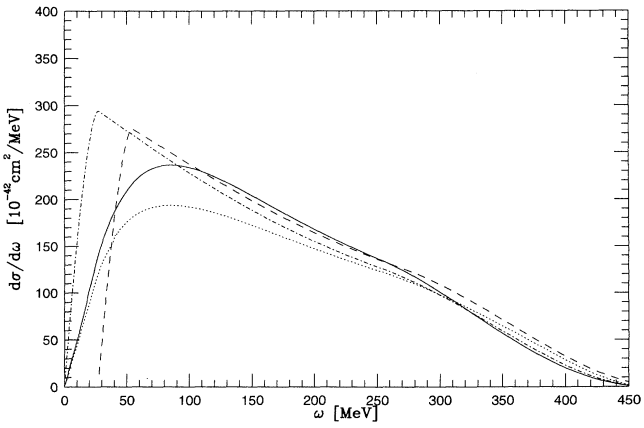

FIG. 2. The response of the ^{16}O nucleus to ν_e's of 600 MeV in a reduced-density nuclear matter calculation. The differential cross section is plotted vs the energy transfer ω. The dot-dashed curve represents the NRFG response calculated without the binding energy correction ($\overline{E}=0$), the dashed curve is the standard NRFG response ($\overline{E}=27$ MeV), the dotted curve is the response with the Landau-Migdal contact potential, and the solid curve is the response for the $\pi+\rho$ exchange + δ-function force.

trons as a function of energy loss ω for a fixed neutrino energy of 600 MeV. Here one can see explicitly how the 27 MeV binding added to the NRFG simulates two-body interactions; both cause the strength to be depleted (compared to the NRFG with no binding) at low energies and enhanced at high energies. The size of this effect is comparable when 27 MeV binding is added to the NRFG and when the force of Eq. (3.1) is used. On the other hand, the pure contact force, which is probably less realistic, depletes considerably more strength from the low-ω region, and adds only a tiny amount at very high ω. The same pattern is present for other neutrino energies as well.

The shift in strength is not hard to understand. The cross section is dominated by the transverse response, in which the pion plays no role. The ρ-exchange piece of Eq. (3.1), which *is* active, is repulsive up to values of q around 770 MeV and hardens the transverse response. The Landau-Migdal force remains repulsive for all values of q and therefore has an even larger effect. These features are reflected in the event rates calculated with the various models, shown in Table III. Since the atmospheric neutrino spectrum weights relatively low values of ω, the event rates are reduced by a shift of strength to higher excitation energies. The reduction caused by the "standard" force is nearly exactly equal to that induced by the 27 MeV shift of the free Fermi-gas response, while the pure Landau-Migdal interaction yields rates that are about 12% smaller. Although the matter of what kind of force to use at such high values of q and ω is still not resolved [28], the Landau-Migdal interaction is near the edge of plausibility, and in nuclear matter we can probably take the spread of values to represent the maximum uncertainty due to our ignorance of nuclear forces in medium.

Even with a perfect force, however, a nuclear matter calculation has to be viewed as schematic. We therefore discuss effects of the residual interaction in a finite volume as well. Here we implement the continuum RPA as in Refs. [29] and [30]. In this approach the basic building blocks are coherent superpositions of continuum creation and bound-state annihilation operators and their Hermitian conjugates. Integro-differential RPA equations for these phonons can be derived and solved, yielding explicit expressions for ground state correlation and transition amplitudes. Technical problems arising from finite range forces are solved by an expansion in Weinberg states [31].

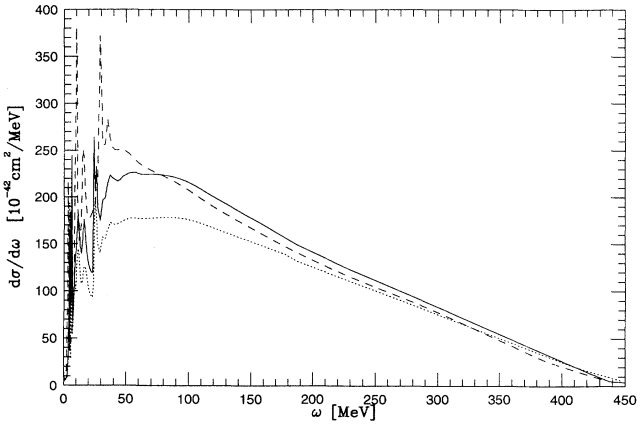

FIG. 3. The response of the ^{16}O nucleus to ν_e's of 600 MeV in a finite-volume calculation. The differential cross section is plotted vs the energy transfer ω. The dashed curve represents the free response (independent nucleons), the dotted curve is the response with the Landau-Migdal contact potential, and the solid curve represents the continuum RPA response calculated with the Bonn meson-exchange G matrix.

Here also, we use two distinct forces to gauge the uncertainty in our calculation. The first is the same pure Landau-Migdal interaction defined in Ref. [27] and used above (though because we are now working in a finite volume, density-dependent terms that have no effect in nuclear matter come into play). The second interaction, of finite range, is a parametrization of the G matrix associated with the Bonn meson-exchange potential [32]. Figure 3 shows cross sections for the two forces, alongside the free Wood-Saxon response, for neutrinos of 600 MeV, as in Fig. 2. A similar though not identical result

TABLE III. The yield ratios of $\mu^- + \mu^+$ and $e^- + e^+$ between the nuclear matter calculation (see text) and the NRFG with binding. Columns 2 and 3 were calculated with the Landau-Migdal force, and columns 4 and 5 with the π and ρ exchange + δ-function force [26].

p (MeV/c)	Nuclear matter/NRFG Landau-Migdal		Nuclear matter/NRFG $\pi+\rho$ exch + δ	
	$\mu^- + \mu^+$	$e^- + e^+$	$\mu^- + \mu^+$	$e^- + e^+$
150	0.87	0.85	0.86	0.84
250	0.89	0.89	0.99	0.98
350	0.90	0.89	1.02	1.02
450	0.88	0.89	1.00	1.00
550	0.88	0.88	0.98	0.98
650	0.88	0.88	0.98	0.97
750	0.88	0.87	0.96	0.96
850	0.87	0.87	0.96	0.96
950	0.87	0.87	0.95	0.95

TABLE IV. The yield ratios of $\mu^- + \mu^+$ and $e^- + e^+$ between the continuum RPA and the free response (i.e., independent nucleons in the Wood-Saxon potential). Columns 2 and 3 were calculated with the Landau-Migdal force, and columns 4 and 5 with the Bonn meson-exchange potential. (*Note that the bin centers are different here.*)

p (MeV/c)	Continuum RPA/free response Landau-Migdal force		Continuum RPA/free response Bonn potential	
	$\mu^- + \mu^+$	$e^- + e^+$	$\mu^- + \mu^+$	$e^- + e^+$
100	0.99	1.07	0.98	1.04
200	0.86	0.87	0.93	0.92
300	0.84	0.84	0.97	0.96
400	0.85	0.85	0.98	0.98
500	0.86	0.87	0.99	0.99

emerges. The Landau-Migdal interaction again depletes the low-energy region and enhances the response very slightly at high energy. The Bonn potential, however, has little effect on the cross section. [This result is consistent with other studies [26], which show that G-matrix calculations tend to yield somewhat less hard-core repulsion than Landau-Migdal parametrizations of low-energy data.] Event rates with the two forces are shown in Table IV. (We were not able to satisfactorily apply our RPA code above a $p_{\rm lep}$ of 500 MeV/c.) The similarities between the entries of Tables III and IV suggest that the magnitude of the effect does not depend sensitively on the size of the nuclear volume.

IV. DISCUSSION

Before summarizing our findings, we must note that several effects not included in this work may alter cross sections and bear investigating. The configurations mixed into the wave functions by our RPA treatment are of the nucleon-hole type. But virtual δ-hole excitations can also admix; the role they play in our process is not yet known. In addition, not all single-ring events need come from quasielastic scattering. Some occur, for instance, when pions are created below Čerenkov threshold, or when two nucleons are ejected from the nucleus. The first effect is included in some approximation in the experimental Monte Carlo codes, but two-nucleon knockout is completely ignored. There is reason [33, 34] to think that one or both of these processes is responsible for excess strength between the quasielastic peak and the δ-knockout region observed in electron scattering [14]. The underlying theory has been developed in several ways, and although no consensus exists on the details, the various methods should be applied to the atmospheric-neutrino problem; at the very least, an additional uncertainty in the rates can be estimated.

Another open problem is the possible modification of nucleon form factors in medium [35, 28]. Again, there is no consensus as to the theoretical foundation for such effects, and little empirical evidence for them in weak processes. However, if the masses M_A and M_V in the vector and axial-vector form factors are reduced by 10–15% as suggested in the cited papers, the cross section in both channels would be reduced by $\approx 20\%$ for all values of $p_{\rm lep}$ we consider.

Apart from all of this, our results in what we consider the most realistic model, the Wood-Saxon well with all the corrections discussed above and the G-matrix-based force, differ only by a few percent from the predictions of the Fermi-gas model for the most important charged-lepton momenta, $p_{\rm lep} \leq 550$ MeV/c. In part the size of the difference is due to a cancellation between, for instance, bound-state and Coulomb effects. In any case, our most important finding is that none of the effects we have considered can possibly alter the μ/e ratio; in Tables I–IV the muon and electron columns are nearly always identical. Our results support the contention that the ratio is a robust measure of the anomaly.

The surprising agreement between our calculated absolute rates and those of the Fermi-gas model carries some uncertainty; the Landau-Migdal interaction reduces the yields by about 13%. An application of that force to the transverse (e, e') response [29], however, leads us to suspect that it underestimates quasielastic neutrino cross sections. In conclusion, then, our results generally support the Fermi-gas model cross sections for purely quasielastic processes in the momentum range relevant to the atmospheric neutrino problem. Whether effects such as two-nucleon knockout or excess pion production increase the cross sections noticeably remains to be seen.

ACKNOWLEDGMENTS

We wish to acknowledge useful discussions with E. Beier, G. Brown, F. Cavanna, M. Ericson, T. K. Gaisser, S. Krewald, and T. Stanev. This work was supported in part by National Science Foundation under Grants Nos. PHY91-08011, PHY90-13248, and PHY91-40397 and by Contract No. DE-F603-88ER-40397 with the U.S. Department of Energy.

[1] K. S. Hirata *et al.*, Phys. Lett. B **205**, 416 (1988); K. S. Hirata *et al.*, *ibid.* **280**, 146 (1992).
[2] R. Becker-Szendy *et al.*, Phys. Rev. D **46**, 3720 (1992).
[3] T. K. Gaisser, T. Stanev, and G. Barr, Phys. Rev. D **38**, 85 (1988); G. Barr, T. K. Gaisser, and Todor Stanev, *ibid.* **39**, 3532 (1989).
[4] M. Honda, K. Kasahara, K. Hidaka, and S. Midorikawa, Phys. Lett. B **248**, 193 (1990).
[5] E. V. Bugaev and V. A. Naumov, Phys. Lett. B **232**, 391 (1989).
[6] J. Lenard *et al.*, Phys. Lett. B **207**, 79 (1988).
[7] V. Barger and K. Whisnant, Phys. Lett. B **209**, 365 (1988).
[8] K. S. Babu and Q. Shafi, Phys. Lett. B **294**, 235 (1992).
[9] W. A. Mann, T. Kafka, and W. Leeson, Phys. Lett. B **291**, 200 (1992).
[10] R. Becker-Szendy *et al.*, Phys. Rev. Lett. **69**, 1010 (1992).
[11] R. A. Smith and E. J. Moniz, Nucl. Phys. **B43**, 605 (1972).
[12] M. Nakahata *et al.*, J. Phys. Soc. Jpn. **55**, 3786 (1986).
[13] R. R. Whitney *et al.*, Phys. Rev. C **9**, 2230 (1974).
[14] P. Barreaau *et al.*, Nucl. Phys. **A402**, 515 (1983).
[15] Z. E. Meziani *et al.*, Phys. Rev. Lett. **54**, 1233 (1985).
[16] C. C. Blatchley *et al.*, Phys. Rev. C **34**, 1243 (1986).
[17] C. R. Chinn, A. Picklesimer, and J. W. Van Orden, Phys. Rev. C **40**, 790 (1989).
[18] B. D. Serot and J. D. Walecka, in *Advances in Nuclear Physics*, edited by J. W. Negele and E. Vogt (Plenum, New York, 1986).
[19] C. J. Horowitz and J. Piekarewicz, Phys. Rev. Lett. **62**, 391 (1989).
[20] K. Wehrberger and F. Beck, Phys. Rev. C **37**, 1148 (1988).
[21] T. Kuramoto, M. Fukugita, Y. Kohyama, and K. Kubodera, Nucl. Phys. **A512**, 711 (1990).
[22] E. V. Bugaev, G. S. Bisnovatyi-Kogan, M. A. Rudzsky, and Z. F. Seidov, Nucl. Phys. **A324**, 350 (1979).
[23] R. Rosenfelder, Ann. Phys. (N.Y.) **128**, 188 (1980).
[24] T. W. Donnelly, Nucl. Phys. **A150**, 393 (1970).
[25] A. L. Fetter and J. D. Walecka, *Quantum Theory of Many-Particle Systems* (McGraw-Hill, New York, 1971).
[26] F. Osterfeld, Rev. Mod. Phys. **64**, 491 (1992).
[27] G. Co and S. Krewald, Nucl. Phys. **A433**, 392 (1985).
[28] G. E. Brown and J. Wambach, report, 1993 (unpublished).
[29] M. Buballa, S. Drozdz, S. Krewald, and J. Speth, Ann. Phys. (N.Y.) **208**, 346 (1991).
[30] E. Kolbe, K. Langanke, S. Krewald, and F. K. Thielemann, Nucl. Phys. **A540**, 599 (1992).
[31] G. Rawitscher, Phys. Rev. C **25**, 2196 (1982).
[32] R. Machleidt, K. Holinde, and Ch. Elster, Phys. Rep. **149**, 1 (1987).
[33] M. J. Dekker, P. J. Brussaard, and J. A. Tjon, Phys. Lett. B **289**, 255 (1992); **266**, 249 (1991).
[34] E. Rost, C. E. Price, and J. R. Shepard, Phys. Rev. C **47**, 2250 (1993).
[35] E. Ruiz Arriola, Chr. V. Christov, and K. Goeke, Phys. Lett. B **225**, 22 (1989); E. N. Nikolov *et al.*, *ibid.* **281**, 208 (1992).